

## A novel method for measuring the radiolysis yields of water adsorbed on ZrO<sub>2</sub> nanoparticles

Jamie S. Southworth, Simon M. Pimblott, Robin M. Orr, Sven P. K. Köhler

Suggested citation:

Southworth, Jamie S., Simon M. Pimblott, Robin M. Orr, and Sven P. K. Köhler. 2020. "A novel method for measuring the radiolysis yields of water adsorbed on ZrO<sub>2</sub> nanoparticles." *Radiation Physics and Chemistry* 174. <https://doi.org/10.25968/opus-2270>.

### Abstract

A novel method has been implemented to prepare metal oxide nanopowders covered with known quantities of adsorbed water; we subsequently studied the  $\gamma$ -radiolysis of ZrO<sub>2</sub> nanopowders covered with H<sub>2</sub>O layers. H<sub>2</sub> yields from the adsorbed water radiolysis are of importance in multiple industrial contexts – the nuclear industry being a prime example. Measured H<sub>2</sub> yields at water coverages of just below and above one monolayer are around 350 times greater than for neat water, but these yields decrease rapidly with increasing water loading of the ZrO<sub>2</sub> nanoparticles, approaching the yield of bulk water at coverages of tens of water layers. The observed plateau of the yields at 0.5 to 2.0 monolayers coverage can be explained by the ease with which electronic excitations in the ZrO<sub>2</sub> can be transferred across the interface to the first one or two adsorbed water layers. However, with increasing water loading, energy transfer to water layers further away from the interface becomes less efficient, and above ~30 water layers, most of the water is not affected by any exciton formation in the ZrO<sub>2</sub>.

### Terms of use

CC BY-NC-ND 4.0

This document is made available under these conditions:  
**Creative Commons - CC BY-NC-ND - Namensnennung - Nicht kommerziell - Keine Bearbeitungen 4.0 International**  
For more information see:  
<https://creativecommons.org/licenses/by-nc-nd/4.0/deed.de>



# A Novel Method for Measuring the Radiolysis Yields of Water Adsorbed on ZrO<sub>2</sub> Nanoparticles

Jamie S. Southworth<sup>a,b</sup>, Simon M. Pimblott<sup>a,b,c</sup>, Robin M. Orr<sup>d</sup> and Sven P. K. Koehler<sup>b,e,\*</sup>

<sup>a</sup> School of Chemistry, The University of Manchester, Oxford Road, Manchester, M13 9PL, UK

<sup>b</sup> Dalton Cumbrian Facility, The University of Manchester, Westlakes Science and Technology Park, Moor Row, CA24 3HA, UK

<sup>c</sup> Idaho National Laboratory, Nuclear Science User Facilities, 995 University Boulevard, Idaho Falls, ID 83401-0355, USA

<sup>d</sup> National Nuclear Laboratory, Sellafield Central Laboratory, Sellafield, Cumbria, CA20 1PG, UK

<sup>e</sup> Department of Natural Sciences, Manchester Metropolitan University, Chester Street, Manchester, M1 5GD, UK

\* Corresponding author: [s.koehler@mmu.ac.uk](mailto:s.koehler@mmu.ac.uk)

## Abstract

A novel method has been implemented to prepare metal oxide nanopowders covered with known quantities of adsorbed water; we subsequently studied the  $\gamma$ -radiolysis of ZrO<sub>2</sub> nanopowders covered with H<sub>2</sub>O layers. H<sub>2</sub> yields from the adsorbed water radiolysis are of importance in multiple industrial contexts – the nuclear industry being a prime example. Measured H<sub>2</sub> yields at water coverages of just below and above one monolayer are around 350 times greater than for neat water, but these yields decrease rapidly with increasing water loading of the ZrO<sub>2</sub> nanoparticles, approaching the yield of bulk water at coverages of tens of water layers. The observed plateau of the yields at 0.5 to 2.0 monolayers coverage can be explained by the ease with which electronic excitations in the ZrO<sub>2</sub> can be transferred across the interface to the first one or two adsorbed water layers. However, with increasing water loading, energy transfer to water layers further away from the interface becomes less efficient, and above ~30 water layers, most of the water is not affected by any exciton formation in the ZrO<sub>2</sub>.

## Keywords

Radiolysis, Zirconia, ZrO<sub>2</sub>, Nanoparticles, Hydrogen Evolution, Exciton Migration

## 1. Introduction

Water radiolysis is a process which has been studied for decades.<sup>1,2</sup> It has important implications in areas as diverse as interstellar chemistry,<sup>3</sup> food sterilisation,<sup>4</sup> as well as in the nuclear industry.<sup>5</sup> The radiolysis of liquid water is a well-defined process, and there is general a consensus as to the yields of the stable products such as  $\text{H}_2\text{O}_2$  and  $\text{H}_2$ .<sup>6</sup>

The radiolysis of condensed water in contact with a solid substrate is also important in a number of areas. Water radiolysis occurs in interstellar space on ice grains (which typically grow on dust particles), and in nuclear environments, where water may be in contact with reactor walls or adsorbed on cladding material or fuel pellets; the adsorbed water is naturally exposed to ionising radiation under those conditions. Radiolysis of adsorbed water gives rise to  $\text{H}_2$  evolution but the yield of  $\text{H}_2$  depends strongly on the identity of the species on which the water molecules are adsorbed.<sup>10</sup> This is because different phases absorb different amounts of energy, and this energy may migrate within one phase, but may also transfer across the interface with varying efficiencies. In particular, the energy migration from phase A to phase B may have a very different efficient than from phase B to A, and this energy redistribution may lead to radiation yields in heterogeneous systems that can differ significantly from those in homogeneous systems.

Increased  $\text{H}_2$  yields from water adsorbed on metal oxides during water radiolysis in the nuclear industry can present significant safety and engineering challenges from the formation of flammable atmospheres, or the alteration of reactor water chemistry, to the corrosion of storage containers or triggering of hydrogen embrittlement of steels.<sup>7,8</sup>

Water can come into contact with spent nuclear fuel (i.e.  $\text{UO}_2$  and  $\text{PuO}_2$ ) during storage, or water vapour from the atmosphere or remnants from the cooling and separation process may adsorb on the oxides. Water may also be in contact with  $\text{ZrO}_2$  from zircalloy cladding in water-cooled reactors. Due to the self-irradiating nature of  $\text{UO}_2$  and  $\text{PuO}_2$  and the multicomponent radiation field present in fuel storage facilities, the radiolysis of adsorbed water under these conditions is a process which requires thorough characterisation. There has hence been an increase in the studies of the radiation-induced chemistry of water adsorbed on or aqueous suspensions of various metal oxides, both active and non-active, in recent years.<sup>9,10,11,12,13,14,15</sup> One of the oxides which has attracted

particular attention is Zirconia ( $\text{ZrO}_2$ ); this is for a number of reasons, but one contributing factor is the remarkably high radiation-catalytic yield of  $\text{H}_2$  from  $\text{ZrO}_2$ -adsorbed water radiolysis.<sup>16,17,18</sup>

Alloys of zirconium are used as fuel rod cladding due to their high thermal conductivity and low neutron capture cross section,<sup>19</sup> meaning water in contact with  $\text{ZrO}_2$  (either in the liquid phase or adsorbed on its surface) is commonplace in the nuclear industry through the use of water cooled/moderated reactors and the ubiquitous nature of water in contaminated waste storage. Therefore, a thorough understanding of the radiation induced chemistry of water adsorbed on  $\text{ZrO}_2$  is required.

In radiation chemistry, yields are conventionally defined as G values, the number of molecules of a species produced or consumed per 100 eV of energy absorbed by the irradiated system.  $G(\text{H}_2)$ , the G value for  $\text{H}_2$  production for water in the presence of a radical scavenger is well documented to be  $\sim 0.45$  molecules/100 eV. A radical scavenger ( $\text{Br}^-$ , from 0.1 mmol KBr) quickly reacts in solution with the OH radical (which would otherwise react with the newly-formed  $\text{H}_2$ ), and the scavenger's presence thus ensures true  $\text{H}_2$  yields are measured.

Previous works by Petrik *et al.* and LaVerne *et al.* have reported a three order of magnitude enhancement in the radiolytic yield of  $\text{H}_2$  for the radiolysis of water adsorbed on  $\text{ZrO}_2$  compared to the yield from neat water in the presence of a radical scavenger.<sup>9,17,18</sup>

The abnormally high radiation-catalytic yield of  $\text{H}_2$  from water adsorbed on  $\text{ZrO}_2$  is observed to become more pronounced as the water coverage decreases, in particular below five monolayers. The quantity of adsorbed water present on a surface can be expressed as the average number of monolayers (MLs). A single ML, defined here as  $10^{15} \text{ cm}^{-2}$ , is said to have formed when each available surface adsorption site is occupied.<sup>20</sup> In reality, the water molecules may not deposit onto a surface in an ordered, perfectly layered fashion, however, the number of water layers is a good indication of water loading.

In the case of  $\text{H}_2$  production from water adsorbed on  $\text{ZrO}_2$ , the G value has been shown to increase from 0.45 (for scavenged water) to greater than 150 molecules/100 eV for less than three MLs of adsorbed water.<sup>21</sup> However, it has not yet been possible to extend this range to coverages below two MLs. It is important to note here that radiation-catalytic yields can be expressed with

respect to the whole chemical system (i.e. metal oxide and water), or with respect to the mass of the water alone. In the data presented here – in agreement with the majority of previous studies – the energy absorbed (and hence the G values) are calculated with respect to the mass of the water only.<sup>21</sup> This procedure shows most clearly any influence that the metal oxide substrate has on the radiation-catalytic yield.

One possible explanation for the enhanced radiation-catalytic yield of H<sub>2</sub> from the decomposition of surface bound water is related to the band gap of ZrO<sub>2</sub>, which is ~5.0 eV.<sup>22</sup> Incident radiation may lead to the formation of excited states within the ZrO<sub>2</sub> crystal (known as excitons – electrostatically bound electron hole pairs), which have an energy of at least the band gap, i.e. ~5.0 eV for ZrO<sub>2</sub>. Migration of these excitons to the surface of the metal oxide can lead to energy transfer from the oxide to the adsorbed water molecules.<sup>23</sup> This is compounded by a close match in energy between the exciton and the dissociation energy of the H–OH bond of adsorbed water, which is ~5.5 eV.<sup>24</sup> This close match not only facilitates energy transfer from the metal oxide to the water, but the energy is also in the desired range to cause dissociation of the adsorbed water, ultimately leading to H<sub>2</sub> production, such that this exciton migration and transfer across the interface may initiate radiolysis processes and may be responsible for the enhanced G(H<sub>2</sub>) values observed during water radiolysis in the presence of ZrO<sub>2</sub>.

One would expect that as the amount of water increases, the yield of H<sub>2</sub> would increase. However, these enhanced G(H<sub>2</sub>) values (calculated per mass of adsorbed water) from adsorbed water radiolysis decrease as the amount of adsorbed water increases.

As exciton migration distances are finite, adsorbed water layers more distant from the oxide interface hence do not experience the effect of the exciton once it transferred from the ZrO<sub>2</sub> to the water. Excitation of the water is most likely for those water layers closest to the ZrO<sub>2</sub>, yet the mass of the outer water layers is considered in dose calculations, thus G values decrease with increasing water loading until they ultimately reach the value for pure water (in the presence of a scavenger) as most of the water molecules do not experience the effect of the ZrO<sub>2</sub> excitation and hence tend towards the G value of pure water.

Since the yields of H<sub>2</sub> production have been fairly well characterised down to one water monolayer, but not below, the results presented here for ZrO<sub>2</sub> with water adsorbed at sub-monolayer coverages are required for a better elucidation of the energy transfer across the oxide/water interface, and a more precise determination of the relevant length scales of energy transfer to condensed-phase water.

Previous investigations which studied the radiation-catalytic yields of water on ZrO<sub>2</sub>, or other oxides, down to a few layers have achieved water adsorption by exposure to a constant Relative Humidity (%RH) in a sealed chamber<sup>14,21</sup> or by introduction of a fixed amount of water vapour.<sup>24</sup> Nominally dry oxide powders are exposed to an atmosphere with a constant %RH content determined by either saturated salt solutions or an acid solution (e.g. H<sub>2</sub>SO<sub>4</sub>) of varying concentration.<sup>25,26</sup> The average number of water layers is then quantified by the change in mass of the sample between pre and post %RH exposure.

However, the relative humidity method does not allow a priori control over the how much water is introduced to the sample. To select the number of water layers, salt solutions must be adjusted in a “trial and error” fashion until desired water coverages are achieved. In practice, water coverages of between three and thirty water layers have been achieved, depending on the nature of the oxide, whereas our newly developed method allows lower coverages to be reached to extend the data range.<sup>21,27</sup> Water adsorption by %RH control also bears the risk of contamination of sample surfaces with species present in the air or humidity control chamber, since the sample is exposed to the atmosphere after baking.

It is hence important that any experiments are performed under as clean and well-defined conditions as possible. The precise number of water layers deposited onto a clean surface must be known for an accurate calculation of the energy deposited, and the capability to deliver pre-selected amounts of water promises an opportunity to better observe the effect of the interface on adsorbed water radiolysis at low water coverages.<sup>24</sup>

This paper thus describes a novel method to prepare adsorbed water on metal oxide nanoparticles using a bespoke vacuum line. The method minimises exposure to air after heat treatment (to drive off excess water) to a minimum, and keeps the nano-powder under vacuum for

cleaner and better-defined conditions. The amount of water to be adsorbed can be pre-selected with sub-monolayer precision and is reproducible. This allows the quantification of radiation yields for water coverages that were previously much more difficult to access. That is, the number of water layers can be finely selected during preparation to below one monolayer. Finally, metal oxide samples can be recovered and re-used at the end of each experimental run.

This preparation method was applied to the  $\gamma$ -radiolysis of water adsorbed on  $\text{ZrO}_2$  to measure  $G(\text{H}_2)$  values in the 0.5 to 5.0 ML range. The species produced under these clean conditions and low adsorbed water layer coverages were quantified by gas chromatography, crucially without the need to open the sample system to the atmosphere between irradiation and measurement.

Experiments were also carried out using the humidity control method of sample preparation. The data obtained from both methods were compared to literature data and were found to be in excellent agreement.

## **2. Experimental**

### *2.1 Sample pre-treatment*

$\text{ZrO}_2$  (99.999%, 20 nm nominal average particle diameter) was procured from Alfa Aesar and used without further purification. The crystal structure was established using a Bruker D8 diffractometer (between  $2\theta$  values of  $20^\circ$  and  $80^\circ$  while the sample was static) and observed to be monoclinic. The specific surface area of a representative sample of the batch was determined by the BET method using a Tristar II surface area analyser and determined to be  $22.5 \pm 0.1 \text{ m}^2/\text{g}$ . The shape of the isotherm and lack of hysteresis loop indicate the non-porosity of the particles. Heat treatment or irradiation up to the maximum dose of 51.14 kGy did not cause any detectable change in crystal structure or specific surface area of the particles.

## 2.2 Humidity Chamber Method

ZrO<sub>2</sub> powder was baked at 400°C for up to 24 h to remove adsorbed water and subsequently cooled in a desiccator at atmospheric pressure at <4 %RH. Within 10-15min, samples were weighed in Pyrex sample tubes (10.0 cm length, 1.0 cm diameter) and placed in a sealed constant humidity chamber for 12-48 hours, depending on desired water uptake. The humidity of the chamber was controlled using saturated salt solutions and the %RH measured using Testo 174H data loggers.<sup>25</sup> After uptake of water, samples were re-weighed, followed by purging the sample tubes with a positive pressure of argon (99.999%, procured from BOC), which only affected the water loading by a few % of a water layer, before being flame-sealed. Control experiments were performed in which empty, purged Pyrex tubes were irradiated, and these did not generate a detectable amount of either H<sub>2</sub> or O<sub>2</sub>. Samples were irradiated using a Foss Therapy Services Inc. 812 self-contained 60-Co radiation source located at the Dalton Cumbrian Facility, The University of Manchester. To analyse the gases produced, the Pyrex sample tubes were broken in a Tygon sampling loop of a specially adapted SRI 8160C Gas Chromatograph (GC) coupled to a Thermal Conductivity Detector (TCD).<sup>12,13</sup>

The drawbacks of this method, which drove the development of the vacuum line method, are: the sample is opened to air multiple times during preparation, i.e. during sample heat treatment, cooling, transfer from %RH chamber to the balance, and prior to purging with Ar, which could introduce contamination to the oxides. Any change in water loading on the oxide surfaces - while potentially small - can still occur during the weighing process on exposure to laboratory air and cannot be quantified. The sample can also be contaminated by species present from the salt or acid solutions during water adsorption by %RH control.

This method is also prone to a high error rate as e.g. analyte gas may be lost if the Pyrex cuts through the Tygon tubing. Most importantly, oxide samples prepared by this method cannot be re-

used as they are contaminated by glass. This method has hence major drawbacks, especially for expensive or rare materials and radioactive substances such as  $\text{PuO}_2$ ,  $\text{UO}_2$  and  $\text{ThO}_2$ .

### 2.3 Vacuum Line Method

Stainless-steel Swagelok vessels (SS-4CS-TW-10) of volume  $10 \text{ cm}^3$  with gas-tight all-metal stop taps (SS-4H), which can be irradiated without forming further radiolysis products, were loaded with  $\text{ZrO}_2$  ( $\sim 1.5 \text{ g}$ ,  $22.5 \text{ m}^2/\text{g}$ ). These were subsequently baked (with the stop taps in the open position) for 24 h at  $400^\circ\text{C}$  and under vacuum ( $\sim 50.0 \text{ mTorr}$ ) to remove adsorbed water and surface contaminants. There may be trace amounts of residual water on the metal oxide surface remaining, or dangling OH bonds from dissociatively chemisorbed water; however, these are below our detection sensitivity, as shown by our irradiation experiments of nominally dry oxide sample surfaces: these yielded no detectable volumes of  $\text{H}_2$ , showing that this drying procedure leads to clean and dry samples for the purpose of this study. Irradiation of empty sample vessels also did not generate any detectable amounts of  $\text{H}_2$  gas. Vials containing powder were cooled to a temperature at which they could be handled using heat proof gloves and stop taps closed immediately upon breaking the oven vacuum. These were then connected to a bespoke Swagelok vacuum line constructed from 316-stainless steel and re-evacuated using a turbomolecular pump (Edwards EXT 75DX) backed by a rotary vane pump (Edwards D4B) to an ultimate pressure of  $\sim 0.4 \text{ mTorr}$ ; a schematic diagram of the vacuum line is shown in Figure 1.

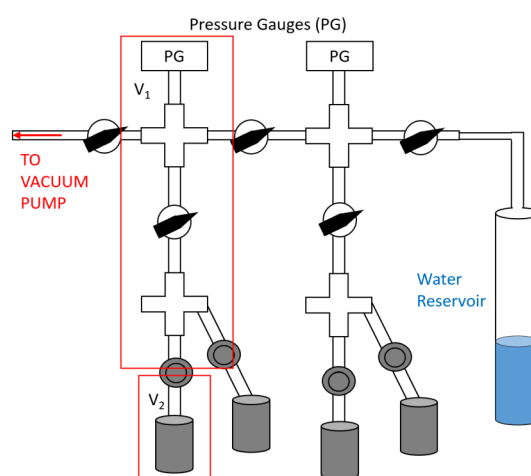


**Figure 1:** Schematic diagram of the vacuum manifold; the system is constructed from all-metal 316 stainless-steel parts and evacuated using a turbomolecular pump backed by a rotary vane pump to an ultimate pressure of 0.4 mTorr to ensure minimal exposure to contaminants during sample preparation.

The system has a leak rate significantly below the rate which would contribute to the gas measurements on the time scale of the experiments. Care was taken when opening the stop taps during evacuation to ensure that the nanopowder is not drawn into the vacuum line. Contamination of the vacuum line was avoided using particle filters (SS-4F-2) mounted above the SS-4H taps, and visual inspection of these filters confirmed that only a negligible amount of nanopowder – if any at all – was removed from the sample vessels. All samples are stored under vacuum when not in use.

Using the labelling from Figure 1, vials containing oxide powder ( $V_2$ ) are evacuated to  $\sim 0.4$  mTorr before being isolated from the vacuum line by closing the all-metal stop tap.  $V_1$  is isolated by closing the relevant taps and the evacuated vacuum line was then connected to a liquid water reservoir; volume  $V_1$  is then filled with approximately 16.0 Torr of water vapour (measured using Kurt Lesker 275i pressure gauges) from the  $H_2O$  reservoir (ultrapure water with a resistivity of 18.2  $M\Omega$  cm and used without further purification). The reservoir was then closed-off from the vacuum line and the vapour pressure in  $V_1$  is allowed to equally distribute in  $V_1$  while  $V_2$  remains evacuated. The water vapour in  $V_1$  is then opened to the sample volume,  $V_2$ . Knowing the volumes of  $V_1$  and  $V_2$  allows the pressure change after re-opening  $V_1$  (now containing water vapour) to the evacuated sample vial,  $V_2$ , in the absence of  $ZrO_2$ , to be calculated. This pressure change was verified in control experiments.

In the presence of  $ZrO_2$  powder, a significantly greater pressure drop was observed while the oxide powder was exposed to the water vapor for between 5 and 20 minutes, when the pressure asymptotically reached an equilibrium value. This pressure drop was attributed to adsorption of water onto the surface of the oxide. Using the mass of the dry sample and its specific surface area, the average number of adsorbed water layers was then calculated from this greater difference in pressure change. In essence, this method for the preparation of nano-powders is a cruder version of the King-Wells method to measure sticking coefficients on single crystals under ultra-high vacuum.<sup>28</sup> Once the desired number of water layers had been adsorbed on the  $ZrO_2$  sample, the vial was briefly re-

evacuated to remove any non-adsorbed water vapour. The water layer range obtained in this way could be chosen to be between 0.5 and five monolayers. We note that we evacuated the vial after water adsorption to not distort our results due to the presence of water vapor, which may also form  $H_2$  radiolytically. Some water from the adsorbed layers will (after evacuation of the vial to  $\sim 0.4$  mTorr) evaporate to re-establish an equilibrium, but we have not measured the corresponding isotherm. However, in a ‘worst case’ scenario, the water vapor pressure after evaporation would be 16 Torr, see above, which in a vessel of  $10\text{ cm}^3$  volume corresponds to  $\sim 5 \times 10^{18}$  water molecules. Since our samples adsorb  $\sim 3 \times 10^{20}$  water molecules per water layer, the introduced error is  $\sim 1.5\%$ . Moreover, adsorption energies for water on  $ZrO_2$  (first layer) are higher than those for consecutive layers (reducing the error further), and the agreement of the  $G$  values at 4 ML coverage and more between the vacuum line method and the relative humidity chamber lend confidence to this method.

To further validate this method, we have also compared the difference in mass of the sample vessel, including sample, stop tap, and adsorbed water, before and after water adsorption on the one hand with the mass increase calculated due to the number of water layers as established by the pressure drop method; this correlation is shown in Figure 2. Due to the excellent agreement, we have in practice only used the pressure drop method due to its quicker application and instantaneous results.

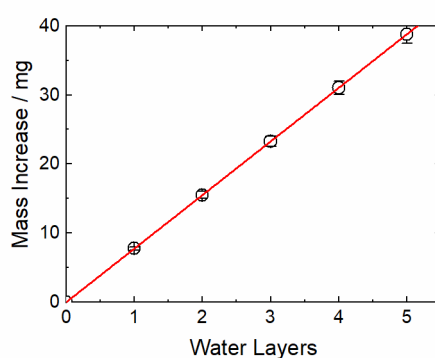


**Figure 2:** Correlation of the mass of adsorbed water with the number of water layers as calculated from the pressure drop method, see text. Errors derived from an average of three measurements and the error associated with the balance.

Evacuated vials were subsequently irradiated at 298 K using  $\gamma$ -rays from the  $60\text{-Co}$  radiation source. We measured the dose rate by Fricke Dosimetry in September 2017 to be 447.8 Gy/min. The gases produced were analysed using a specially adapted SRI 8610C GC coupled to a TCD by directly

mating the sample vessels to the GC and evacuating the pipework in-between (before opening the stop taps) to exclude any errors potentially being introduced by the presence of atmospheric gases. The narrow width of the detected peaks confirms the prompt and complete injection using this method. The carrier gas determines the sensitivity of the TCD to the analyte gas. Argon (99.999%) was selected as the carrier in this case due to H<sub>2</sub> and Ar having significantly different thermal conductivities. Gas concentrations were extracted from the integrated GC signals for each respective gas.

The main benefits of this vacuum method over the humidity control chamber method are: 1) sub-monolayer coverages on the sample surface can be achieved; 2) water coverages can be pre-selected rather than having to be established after exposure in a relative humidity chamber; 3) the vacuum line method also minimises sample contact with air, ensuring cleaner conditions; 4) samples can be recovered after each experiment.

### **3. Results and Discussion**

#### *3.1 Humidity Chamber Method*

Figure 3 shows the number of H<sub>2</sub> molecules as a function of the energy absorbed by the water adsorbed on the ZrO<sub>2</sub> only. The large errors associated with the data points take into account the errors introduced during calibration of the GC (estimated to be 7%) arising from the difference in integrated peak area when injecting three identical volumes of calibration gas, but are also due to increasing G values as the water loading decreases during experiments.

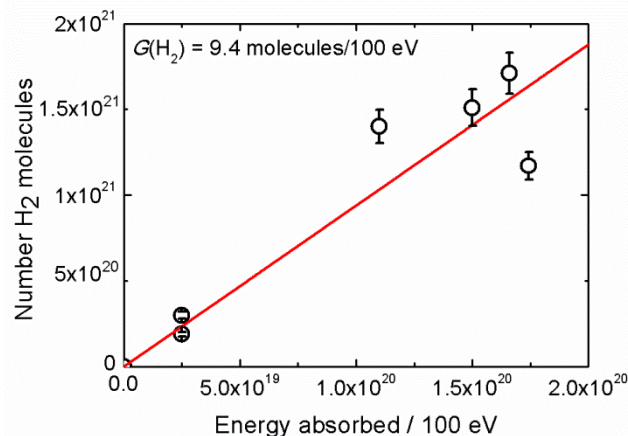


**Figure 3:** Number of molecules of H<sub>2</sub> produced as a function of the energy absorbed from the <sup>60</sup>Co  $\gamma$ -ray radiolysis of eight monolayers of water adsorbed on ZrO<sub>2</sub> (1.0 g, 22.5 m<sup>2</sup>/g). Absorbed energy calculated with respect to the mass of the adsorbed water only. Note the unit of the abscissa of 100 eV – the slope of the linear best fit then directly yields the G(H<sub>2</sub>) value.

The yield of H<sub>2</sub> appears to be roughly linear with respect to energy absorbed up to the maximum dose in this series of experiments, 36.5 kGy. As is clear from the plot, the data has a large amount of scatter. Water adsorption to oxide samples by the %RH method introduces a range of errors, not all of which can be quantified. The errors that are quantified and included in the plot are the error associated with the balance, the change in sample mass when open to atmosphere, and the error associated with the thermal conductivity detector.

Figure 4 shows the variation in G(H<sub>2</sub>) with the number of adsorbed water layers when the samples are prepared by the humidity chamber method. The results show that as the number of water layers increases, G(H<sub>2</sub>) sharply decreases. These yields approach those expected for pure water as the number of water layers exceeds ~30. This is because the (now dominating) outer water layers may simply undergo direct radiolysis without experiencing any effect from the interface as they are simply too far removed from the interface.

It is worth noting that those lower yields for higher coverages do not indicate that less H<sub>2</sub> is formed, but since the yields are calculated with respect to the mass of the adsorbed water (which increases with increasing number of water layers), the radiation yields decrease as the amount of H<sub>2</sub> formed increases at a slower rate than the mass of the adsorbed water.

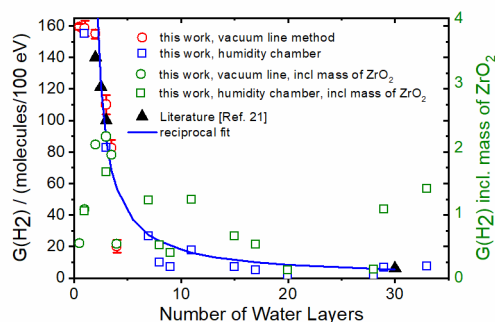


**Figure 4:**  $G(\text{H}_2)$  values plotted as a function of the number of water layers adsorbed on  $\text{ZrO}_2$  and compared to literature data taken from Ref. 21. Red open circles ( $\circ$ ) represent data recorded using the vacuum line method to prepare 0.5 to 5 monolayers of adsorbed water. Energy absorbed is calculated with respect to the mass of the adsorbed water only. Blue open squares ( $\square$ ) represent data obtained using the humidity control method, and literature data by LaVerne *et al.* [Ref. 21] is shown as closed black triangles ( $\blacktriangle$ ). The blue line is an offset reciprocal fit to all red and blue data points. Green data points  $\circ$  and  $\square$  are the same data, but  $G$  values are calculated with respect to the mass of the whole system ( $\text{ZrO}_2$  substrate and adsorbed water).

The maximum  $G(\text{H}_2)$  value observed using the humidity chamber method was  $158.5 \pm 10.9$  molecules/100 eV and was observed for one monolayer of water. The effect of the oxide can be clearly seen to diminish rapidly within the first five monolayers of adsorbed water, and by ten monolayers,  $G(\text{H}_2)$  has decreased more than an order of magnitude. While we have managed to record  $G(\text{H}_2)$  values for the range between  $\sim 5$  and 30 monolayers using the relative humidity chamber, there is still a lack of both literature and our own data at below 5 monolayers, especially in the crucial region just above and below one monolayer.

The large errors associated with the experimental results presented in Figure 4 arise – amongst others – from uncertainties introduced when the sample is exposed to the atmosphere during the preparation process (such as when moving the sample from the relative humidity chamber to record its mass). This gives rise to an average error of  $\pm 5$  molecules/100 eV. Hence, when measuring a small  $G(\text{H}_2)$  values, the uncertainty can be significant.

### 3.2 Vacuum Line Method

Figure 5 shows the amount of  $\text{H}_2$  (expressed as the number of molecules) produced from similar oxide samples (i.e. with identical water loading) as a function of radiation dose using the vacuum line method. It is clear that the yield linearly increases with absorbed energy, within error, up

to 51.1 kGy, the maximum dose in these experiments, as expected, and that the vacuum line method gives rise to a smaller error as compared to the relative humidity chamber method, see Fig. 3. Unirradiated samples with adsorbed water, left under vacuum for an extended period of time, did not yield any H<sub>2</sub>. Further experiments (not shown) have established that yields are only a function of the dose, but *not* the dose rate.

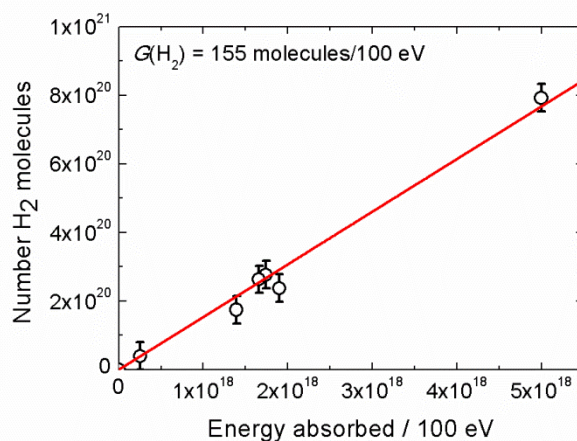


**Figure 5:** Number of molecules of H<sub>2</sub> produced as a function of energy absorbed for 2 monolayers of water adsorbed on the surface of ZrO<sub>2</sub> (1.5 g, 22.5 m<sup>2</sup>/g). Note the units on the abscissa (per 100 eV) such that G values can be extracted directly from the slope of the linear best fit.

As previously stated, the absorbed dose is calculated with respect to the mass of the water only and not to the whole metal oxide/water system for two reasons: 1) It is in agreement with most previous work in the literature; 2) more importantly, it shows most clearly any potential influence from the oxide substrate. If the metal oxide substrate did not have an effect on the production of H<sub>2</sub>, then the radiolytic yield calculated for the energy absorbed by the mass of the adsorbed water only would be approximately the yield for water (~0.45 molecules/100 eV for radically scavenged water); any deviation from this G(H<sub>2</sub>) value can now be attributed to the presence of the oxide.

Figure 4 also includes the G(H<sub>2</sub>) values obtained using the vacuum line method, shown against data from the corresponding humidity chamber experiments and results by LaVerne and co-workers using a variation of the humidity chamber method.<sup>12,13,29</sup> One can see from Figure 4 that the yields obtained employing the vacuum line method overlap with those obtained using the humidity chamber method, giving confidence in our methodology. More importantly, the vacuum method

reduces errors, evenly covers the range up to five MLs, and extends the range of water coverages for which yields have been obtained to below one monolayer.

Figure 4 also shows an apparent plateau between 0.5 and 2 monolayers of water coverage, followed by a steep decrease in yields between two and five water layers, followed by the radiation yields  $G(\text{H}_2)$  slowly approaching the bulk value for water of 0.45 molecules/100 eV at even higher coverages.

These three features (plateau around 1 ML, steep decrease, and levelling off around 0.45 molecules/100 eV) are all consistent with the previously suggested mechanism involving bulk exciton formation followed by exciton migration to the interface, currently the most widely accepted mechanism explaining the enhanced  $\text{H}_2$  yields compared pure water. More specifically, excitons are created within the oxide (or on the surface of the  $\text{ZrO}_2$ ) from where they migrate to the surface; due to the close match of the exciton energy (at or above the band gap of the substrate,  $\sim 5.0$  eV for  $\text{ZrO}_2$ ),<sup>22</sup> and the water dissociation energy, the exciton energy can transfer across the interface to the water; the close match with the H–OH bond dissociation energy can then cause water dissociation, leading to  $\text{H}_2$  production. The release of energy upon exciton relaxation can then trigger the dissociation of adsorbed species.<sup>9,24</sup>

The yields which approach values close to those for pure water at coverages from above around  $\sim 20$  water layers can be explained by the finite migration distance of excitons through water. Since water layers far away from the oxide substrate do not experience the influence of the substrate, the radiation chemical yield of these outer layers is close to that for water, and since the abundance of water far enough away from the interface increases with increasing coverage, the decline of the  $G(\text{H}_2)$  value towards 0.45 molecules/100 eV is expected.

At between 0.5 and 1.5 monolayers,  $G(\text{H}_2)$  is around 158 molecules/100 eV with little variation. This means that since the mass of water increases three-fold (and absorbed dose is calculated with respect to the mass of the water), but radiation yields are the same, the amount of  $\text{H}_2$  produced from 1.5 MLs of water is three times more than that at 0.5 MLs. Firstly, this indicates that the number of excitons *in the oxide* exceeds the number of water molecules as the number of water molecules limits the yield, i.e. our results show that roughly the same number of  $\text{H}_2$  molecules are

produced as H<sub>2</sub>O molecules are initially adsorbed, and for twice the amount of water adsorbed, twice as much H<sub>2</sub> is detected. Secondly, it also implies that exciton transfer is equally efficient to every water molecule in the first shell, and evidently also for part of the second shell.

To support the theory that additional MLs of water molecules do not experience the effect of exciton formation in the solid to the same extent, a reciprocal function relating the observed yields G(H<sub>2</sub>) to the number of monolayers has been fitted; this reciprocal fit is shown as the solid curve in Figure 4. We have chosen a reciprocal function (to fit both our two experimental data sets and literature data) slightly offset to account for the fact that for coverages of 0.5, 1 and even 2 layers of water, the G values barely change, indicating that energy transfer from the nanoparticle to any water molecule in the first two shells is roughly equally likely. The sharp drop in radiation yields with increasing water coverages for the ZrO<sub>2</sub>/H<sub>2</sub>O system has been observed previously.<sup>29</sup>

#### 4. Conclusion

This work reports H<sub>2</sub> yields from the  $\gamma$ -radiolysis of water adsorbed on ZrO<sub>2</sub> nanopowders by two different methods. The yields are highest at low water loading (between 0.5 and 1.5 monolayers of water on the ZrO<sub>2</sub> surface), indicating an efficient energy transfer from the oxide to the adsorbed water, but the yields decrease with increasing water loading, approaching the bulk value of 0.45 molecules/100 eV at tens of monolayers.

Those higher water loadings were realised using the previously employed humidity chamber method, while coverages with four or fewer water layers were realised using the vacuum line method, which had not been applied to ZrO<sub>2</sub> nanopowders previously. This technique allows precise control over the quantity of water adsorbed onto a clean oxide surface, and kept the oxide under clean and well defined conditions throughout. It also allowed us to expand the range of water coverages to below one monolayer. The experimental results using the new method thus focus on between 0.5 and four water layers where the effect of the surface on the radiation yields is felt the strongest.

This work allowed us to better characterise the energy transfer process across the ZrO<sub>2</sub>/H<sub>2</sub>O interface which is of fundamental importance in nuclear reactor safety, and relevant to nuclear waste storage and incident prevention. The better control which this novel method allowed helped in

understanding processes underpinning phenomena such as enhanced H<sub>2</sub> production from metal oxides relevant to the nuclear industry.

## Acknowledgments

J.S.S. thanks the UK National Nuclear Laboratory for funding through an EPSRC iCASE studentship.

The authors thank Robin Orr and Howard Sims for helpful discussions.

## Funding

This research was funded by EPSRC and the Dalton Cumbrian Facility project, a joint collaboration of the UK Nuclear Decommissioning Authority and The University of Manchester.

**Data Availability Statement:** The raw data required to reproduce these findings are available to download from Mendeley.

## References

- 
- <sup>1</sup> Allen, A. O.; Radiation Chemistry of Aqueous Solutions, *J. Phys. Chem.*, **1948**, *52*, 479–490
  - <sup>2</sup> Burton, M.; Radiation Chemistry, **1946**, *51*, 611-625
  - <sup>3</sup> Johnson, R. E.; Photolysis and Radiolysis of Water Ice on Outer Solar System Bodies, *J. Geophys. Res.*, **1997**, *102*, 10985-10996
  - <sup>4</sup> Farkas, J.; Irradiation for Better Foods, *Trends in Food Science & Technology*, **2006**, *17*, 148-152
  - <sup>5</sup> Le Caër, S.; Water Radiolysis: Influence of Oxide Surfaces on H<sub>2</sub> Production under Ionizing Radiation, *Water*, **2011**, *3*, 235-253
  - <sup>6</sup> Spinks, J. W. T.; Woods, R. J.; An Introduction to Radiation Chemistry, 3rd Edition, John Wiley & Sons, Inc, New York, **1964**, 39-77
  - <sup>7</sup> Chohan, U. K.; Jimenez-Melero, E.; Koehler, S. P. K.; Surface Atomic Relaxation and Magnetism on Hydrogen-Adsorbed Fe(110) Surfaces from First Principles, *Appl. Surf. Sci.*, **2016**, *387*, 385
  - <sup>8</sup> Chohan, U. K.; Koehler, S. P. K.; Jimenez-Melero, E.; Diffusion of Hydrogen into and through  $\gamma$ -iron by Density Functional Theory, *Surf. Sci.*, **2018**, *56*, 672-673
  - <sup>9</sup> Aleksandrov, A. B.; Bychkov, A. Yu.; Vall, A. I.; Petrik, N. G.; Sedov, V. M.; Radiolysis of Adsorbed Species, *Russ. J. Phys. Chem.*, 1991, *65*, 1604-1608
  - <sup>10</sup> Sims, H. E.; Webb, K. J.; Brown, J.; Morris, J.; Taylor, J. R.; Hydrogen Yields from Water on the Surface of Plutonium Dioxide, *J. Nuc. Mater.*, **2013**, *437*, 359-364
  - <sup>11</sup> LaVerne, J. A.; Tonnie, S. E.; H<sub>2</sub> Production in the Radiolysis of Aqueous SiO<sub>2</sub> Suspensions and Slurries, *J. Phys. Chem. B*, **2003**, *107*, 7277-7280

- 
- <sup>12</sup> Reiff, S. C.; LaVerne, J. A.; Radiation-Induced Chemical Changes to Iron Oxides, *J. Phys. Chem. B*, **2015**, *119*, 7358-7365
- <sup>13</sup> Reiff, S. C.; LaVerne, J. A.; Gamma and He Ion Radiolysis of Copper Oxides, *J. Phys. Chem. C*, **2015**, *119*, 8821-8828
- <sup>14</sup> LaVerne, J. A.; Tandon, L.; H<sub>2</sub> Production in the Radiolysis of Water on UO<sub>2</sub> and Other Oxides, *J. Phys. Chem. B*, **2003**, *107*, 13623-13628
- <sup>15</sup> Reiff, S. C.; LaVerne, J. A.; Radiolysis of Water with Aluminium Oxide Surfaces, *Rad. Phys. Chem.*, **2017**, *131*, 46-50
- <sup>16</sup> Skotnicki, K.; Bobrowski, K.; Proton Transfer of Guanine Radical Cations Studied by Time-Resolved Resonance Raman Spectroscopy Combined with Pulse Radiolysis, *J. Radioanal. Nucl. Chem.*, **2015**, *304*, 473-480
- <sup>17</sup> Roth, O.; Dahlgren, B.; LaVerne, J. A.; Radiolysis of Water on ZrO<sub>2</sub> Nanoparticles, *J. Phys. Chem. C*, **2012**, *116*, 17619-17624
- <sup>18</sup> LaVerne, J. A.; *J. Phys. Chem. B*, H<sub>2</sub> Formation from the Radiolysis of Liquid Water with Zirconia, **2005**, *109*, 5395-5397
- <sup>19</sup> Hallstadius, L.; Johnson, S.; Lahoda, E.; Cladding for High Performance Fuel, *Prog. Nucl. Energ.*, **2012**, *57*, 71-75
- <sup>20</sup> Attard, G.; Barnes, C.; Surfaces, *Oxford University Press*, **1998**, *59*, 5-7
- <sup>21</sup> LaVerne, J. A.; Tandon, L.; H<sub>2</sub> Production in the Radiolysis of Water on CeO<sub>2</sub> and ZrO<sub>2</sub>, *J. Phys. Chem.*, **2002**, *106*, 380-386
- <sup>22</sup> Emeline, A.; Kataeva, G.; Litke, A.; Rudakova, A.; Ryabchuk, V.; Serpone, N.; Spectroscopic and Photoluminescence Studies of a Wide Band Gap Insulating Material: Powdered and Colloidal ZrO<sub>2</sub> Sols, *Langmuir*, **1998**, *14*, 5011-5022
- <sup>23</sup> Caffrey, J. M.; Allen, A. O.; Radiolysis of Pentane in the Adsorbed State, **1958**, *62*, 33-37
- <sup>24</sup> Petrik, N. G.; Alexandrov, A. B.; Vall, A. I.; Interfacial Energy Transfer during Gamma Radiolysis of Water on the Surface of ZrO<sub>2</sub> and Some Other Oxides, *J. Phys. Chem. B*, **2001**, *105*, 5935-5944
- <sup>25</sup> Young, J. F.; Humidity Control in the Laboratory using Salt Solutions – a Review, *J. Appl. Chem.*, **1967**, *17*, 241-245
- <sup>26</sup> Wilson, R. E.; Humidity Control by means of Sulphuric Acid Solutions, with Critical Compilation of Vapour Pressure Data, *Ind. Eng. Chem.*, **1921**, *13*, 326-331
- <sup>27</sup> Southworth, J. S.; Koehler, S. P. K.; Pimblott, S. M.; Gas Production from the Radiolysis of Water Adsorbed on ZnO Nanoparticles, *J. Phys. Chem. C*, **2018**, *122*, 25158-25164
- <sup>28</sup> King, D. A.; Wells, M. G.; Molecular Beam Investigation of Adsorption Kinetics on Bulk Metal Targets: Nitrogen on Tungsten, *Surf. Sci.*, **1972**, *29*, 454-482
- <sup>29</sup> Roth, O.; Dahlgren, B.; LaVerne, J. A.; Radiolysis of Water on ZrO<sub>2</sub> Nanoparticles, *J. Phys. Chem. C*, **2012**, *116*, 17619-17624